Pergamon

PII: S0967-0645(96)00042-2

Deep-Sea Research II, Vol. 43, No. 7–8, pp. 1793–1822, 1996

0967-0645/96 $15.00 + 0.00

Trophodynamic and advective influences on Georges Bank larval cod and haddock

FRANCISCO E. WERNER,* R. IAN PERRY,† R. GREGORY LOUGH‡ and CHRISTOPHER E. NAIMIE§

(*Received* 18 *October* 1994; *in revised form* 1 *February* 1996; *accepted* 14 *May* 1996)

Abstract—Using a model-based approach, the relative effects of advective and trophodynamic (feeding and growth) processes are considered on populations of larval cod (*Gadus morhua*) and haddock (*Melanogrammus aeglefinus*) on Georges Bank. Building on previous studies that describe the role of advection, this study incorporates trophodynamic relationships to examine starvation mortality and growth rates at the level of individual larvae on the Bank. Estimates of prey concentrations and flow fields appropriate for late winter/early spring are used. Both trophodynamic processes and advection influence larval losses from the Bank where, in the absence of starvation, advective losses are on the order of one-fifth of the eggs and larvae spawned on the Bank. Starvation is most important in the first feeding larvae and is much reduced for older larvae. The contact rates between larval fish and zooplankton prey when turbulence is included are 2–5 times greater than the contact rates with no turbulence, and allow the model cod larvae to achieve growth rates similar to those observed on the Bank, although mean rates for larval haddock are still lower than observed. Turbulence-enhanced contact rates are thus determined to be a necessary component in our description of the growth of cod and haddock larvae on Georges Bank. Model cod larvae with growth rates comparable to those observed in the field are located below the surface layer (deeper than 25 m) and inside the 60 m isobath. The region of highest retention due to circulation processes (Werner *et al.*, 1993; *Fisheries Oceanography*, **2**, 43–64) coincides with the region of highest growth rates and highest larval survival. Therefore, there is a complementary interaction between trophodynamic and circulation processes, with those larvae most likely to remain on the Bank also being those in the most favorable feeding regions. Haddock larvae require higher prey densities than cod larvae to survive. Copyright © 1996 Elsevier Science Ltd

1. INTRODUCTION

Hjort (1914) identified recruitment variability as a major cause of fluctuations in marine fish populations, and outlined two hypotheses accounting for this variation. His first hypothesis stated that recruitment variation is regulated by food limitation of the larval stages, while his second hypothesis stated that recruitment variation is regulated by the supply of larvae (mediated by the physical circulation) to or from their appropriate distributional area. Eighty years after Hjort's paper, active debate continues as to which hypothesis is the more important cause of variability in year-class strength of marine fish populations (e.g. Sinclair, 1988; Mullin, 1993). These hypotheses have been examined for cod and haddock larvae on

* Marine Sciences Program, CB no. 3300, University of North Carolina, Chapel Hill, NC 27599-3300, U.S.A.
† Pacific Biological Station, Department of Fisheries and Oceans, Nanaimo, British Columbia, Canada V9R 5K6.
‡ National Marine Fisheries Service, Northeast Fisheries Science Center, Woods Hole, MA 02543, U.S.A.
§ Dartmouth College, Hanover, NH 03755, U.S.A.

Georges Bank, with evidence suggesting food limitation at certain times and for certain areas (e.g. Buckley and Lough, 1987). Other studies suggest that advection of larvae off the Bank is limited by the gyral circulation and the development of frontal zones on the northern and southern flanks (e.g. Smith and Morse, 1985). However, these two processes have rarely been examined simultaneously, perhaps because they represent processes occurring on different spatial scales (Mullin, 1993; Perry, 1994).

Modeling provides a tool for the integration of processes occurring at the scales of individual larvae (i.e. feeding and growth) with processes occurring at the scales of populations and broad circulation features. Studies of Werner *et al.* (1993) and Lough *et al.* (1994) focused on the circulation on Georges Bank as it affects the distribution and transport of larvae spawned on the Bank. They identified a range of conditions (strength of physical forcing, spawning location, position in the water column) that result in larvae being retained on the Bank or advected to neighboring regions (and therefore lost from the Georges Bank system). For example, Werner *et al.* (1993) identified that larvae below the surface Ekman layer and shoalward of the 60–70 m isobaths had higher probabilities of retention on the Bank during spring, while Lough *et al.* (1994) examined the effects of interannual variability in wind conditions coupled with variability of the Scotian Shelf inflow. However, these physically-dominated models included larval growth only as a deterministic function of time, and did not consider the potential for variable larval growth conditions (e.g. prey distributions) about the Bank.

In this paper, we develop an individual-based model (IBM) of the feeding and growth of Atlantic cod and haddock larvae coupled to a three-dimensional circulation model on the realistic topography of Georges Bank. This model allows us to consider Hjort's two hypotheses simultaneously, to examine the feeding, growth, and starvation mortality of larvae on the Bank in the context of their advection along and off of Georges Bank by the circulation. The essence of individual-based models is a recognition that biological entities are not all equal (e.g. Mangel and Clark, 1988; DeAngelis and Gross, 1992), and that variation can occur in egg quality, hatch size, prey encounter rates, prey capture success, predation risk, etc. Variation at each stage affects the ability of individuals to feed, grow, and survive. As a result, for example, the final frequency distribution of the sizes of survivors can be significantly (and nonlinearly) different from the initial size distribution. In addition, using the circulation model to move larvae about the Bank creates a "spatially explicit IBM" (e.g. Tyler and Rose, 1994), since it provides a spatial variation in the encountered prey field and therefore another source of variability among the larvae.

Recent theoretical studies suggest that small-scale turbulence is a significant component in the encounter rate between a larval fish predator and its planktonic prey (Rothschild and Osborn, 1988; MacKenzie and Leggett, 1991; MacKenzie *et al.*, 1994). Spatially and temporally varying turbulence and turbulent kinetic energy dissipation rates associated with features such as the surface and bottom Ekman layers, the pycnocline, and tidal fronts are derived from a circulation model. In this paper we examine the potential importance of incorporating the turbulent kinetic energy dissipation rate into the estimates of larval fish–prey encounter rates for Atlantic cod and haddock feeding and growth on Georges Bank.

2. PREY FIELD

A critical input to the trophodynamic model is the distribution and concentration of prey for the larval cod and haddock. The concentrations of zooplankton prey and their

distributions on Georges Bank used in our study were determined from the literature. Kane (1984) identified the various life-history stages of *Pseudocalanus minutus*, *Calanus finmarchicus*, *Oithona similis*, and *Centropages* sp. as the dominant components of the diets of larval cod and haddock on Georges Bank. Our specification of the prey field concentrates on these four taxonomic groups. Kane (1984) noticed that phytoplankton remains occurred in the guts of smaller larvae, and Gallager and von Herbing (1994) also found microzooplankton in larval cod stomachs, but the importance of these prey items and their nutritive value is unclear. Georges Bank was separated into northern flank (NF), eastern flank (EF), southern flank (SF) and central cap (CC; depths less than 40 m) regions (Fig. 1) based on Davis (1984a). Densities of copepod eggs were assigned equitably to each region using bank-wide mean abundance estimates from springtime observations reported in Laurence (1985). No data are available in the literature to support finer spatial resolution of egg concentrations. However, data on copepod nauplii reported by Davis (1982), based on collections using 0.053 mm mesh nets, provide an estimate of the spatial distribution of nauplii (mean abundance ratios α_i of 0.03:0.38:0.20:0.39 for regions $i = 1,\ldots, 4$, northern flank, eastern flank, southern flank, and central cap, respectively). Copepod nauplii

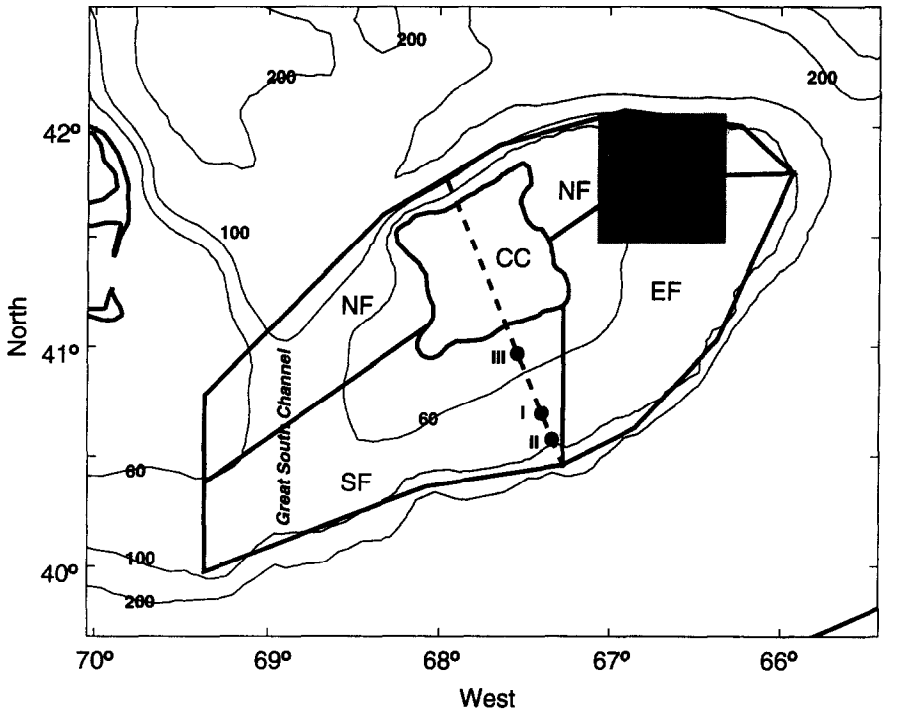

Fig. 1. Georges Bank bathymetry (m) and prey field sectors. The northern flank (NF), the eastern flank (EF), the southern flank (SF) and central cap (CC) prey regions/sectors are outlined; the spawning grounds, located on the Northeast Peak, are indicated by the shaded square. The outline of the Central Cap is defined by the 40 m isobath. The dashed line indicates the section along which values of turbulent kinetic energy dissipation are shown in Fig. 11. Time-histories and vertical profiles of model variables at Sites I, II and III are shown in Figs 12–14; Sites I, II and III correspond to those of Buckley and Lough (1987).

concentrations were therefore calculated for each region $\bar{x}_i$ using the bank-wide mean abundance estimate ($\bar{x}$) reported in Laurence (1985) weighted by the proportion (α_i) sampled by Davis (1982) and the proportion (β_i) of the total area of Georges Bank comprised by the ith region (β_i = 0.21:0.27:0.38:0.13, respectively, for regions i = 1,..., 4), i.e. $\bar{x}_i = \bar{x} \cdot \alpha_i / \beta_i$.

Stage-specific copepodite concentrations were estimated for each region from the observations of *Pseudocalanus* distributions in February 1975 recorded by Davis (1982, 1984a). The additional major prey items (*Calanus finmarchicus*, *Oithona similis*, *Centropages* sp.) were included using the counts for these species in Davis (1982) and assuming that *C. finmarchicus* and *O. similis* had the same life-stage proportions as *Pseudocalanus*. This assumption is most appropriate for *C. finmarchicus* (with a similar life-history strategy on Georges Bank as *Pseudocalanus*, e.g. Davis, 1987) and is reasonable as a first assumption (in the absence of more detailed data) for *O. similis*, which appears to show no strong seasonality on Georges Bank (e.g. Davis, 1987). Comparison of the concentrations of each major prey species presented in Davis (1982) for February 1975 and March–April 1976 using analysis of variance indicated that only *Centropages* sp. stages C3–C6 were significantly (p = 0.048) different between time periods, with abundances in February higher than in March–April. However, *Centropages* sp. stages C3–C6 comprised only 4% of the abundance of the major prey items; therefore this variation was relatively inconsequential to overall prey densities between time periods. We used the February 1975 data for the prey distributions since they had the most complete spatial coverage. Off-bank prey abundances were set to zero because the copepod concentrations for these areas were extremely low (Davis, 1982, 1984a) and our purpose was to model the growth of fish larvae on the Bank. The size ranges (length) and weights of prey were taken from Davis (1984b) for *Pseudocalanus*, with weights in μg C converted to μg dry weight by assuming that carbon comprised 45% of copepod dry weight (Parsons *et al.*, 1984). However, Kane (1984) determined that eggs of *Calanus finmarchicus* were the dominant component of the egg prey category for larval cod and haddock. This is because eggs of *C. finmarchicus* are free-floating, whereas *Pseudocalanus* females retain their eggs (and so free eggs are generally unavailable as prey to early fish larvae). We therefore used the weights of *C. finmarchicus* eggs from Davis (1984b) (adjusted to dry weight as above) as the weight of our egg prey category (Table 1). For nauplii, data in Kane (1984) show that only copepod nauplii > 0.25 mm length (stages N3–N6) occurred in the stomachs of larval cod and haddock. We therefore used the mean weights of this size range of *Pseudocalanus* and *C. finmarchicus* nauplii stages from Davis (1984b) (adjusted to dry weight) as the weight for the nauplii prey category.

Table 1 summarizes the larval fish prey sizes and weights, and the assigned concentrations within each of the four regions on Georges Bank. These distributions were prescribed as time-invariant within each region. Although we recognize this is an artificial constraint, it is justified as a first simplifying assumption based on the ANOVA results described above, which indicated relatively little difference in regional abundances of major prey items between February and March–April. Additionally, we assumed that larval fish feeding had no impact on prey abundance or distribution (e.g. Cushing, 1983). We further assumed that prey concentrations were vertically homogeneous within each region, consistent with the absence of persistent vertical stratification at this time of year.

Table 1. *Zooplankton prey type, mean size (length), mean weight (dry weight) of each size class (based on* Pseudocalanus minutus; *Davis, 1984b), and assigned concentrations within each of the four regions on Georges Bank (northern flank, eastern flank, southern flank, central cap)*

Prey type	Size (mm)	Weight (μg dry wt)	N. flank (no. l^{-1})	E. flank (no. l^{-1})	S. flank (no. l^{-1})	C. cap (no. l^{-1})
Eggs	<0.13	1.60	2.14	2.14	2.14	2.14
Nauplii	0.28	1.20	1.08	12.30	6.36	12.78
C-I	0.42	1.10	0.05	0.49	0.22	0.62
C-II	0.52	1.82	0.05	0.32	0.24	0.35
C-III	0.62	2.89	0.02	0.08	0.22	0.12
C-IV	0.73	4.80	0.04	0.08	0.27	0.11
C-V	0.88	9.58	0.04	0.07	0.31	0.11
C-VI	>0.88	16.67	0.18	0.11	0.24	0.06

Egg and nauplii concentrations calculated as described in the text. Concentrations of copepodites and adults are based on stage-specific distributions of *Pseudocalanus minutus*, but include contributions from *Oithona similis*, *Centropages* sp., and *Calanus finmarchicus* (calculated from data in Davis, 1982).

3. PHYSICAL MODEL FLOW FIELD

A complete description of the three-dimensional, free-surface, fully-nonlinear, prognostic (evolving baroclinic field), finite element hydrodynamic model employed can be found in Lynch *et al.* (1996). The model operates in tidal time and uses the quasi-equilibrium version of Mellor–Yamada level 2.5 turbulence closure scheme (Mellor and Yamada, 1982 and Galperin *et al.*, 1988), by including the turbulent kinetic energy ($q^2/2$) and mixing length (l) as hydrodynamic state variables that are functions of position and time.

The circulation field we computed corresponds to climatological March–April conditions, consistent with the spawning and early larval drift period of cod and haddock on Georges Bank. Initial conditions were based on the M_2 tide and the mean circulation, density, and wind fields described by Naimie *et al.* (1994) for the March–April bimonthly period. The computation included boundary forcing from the M_2 tide, surface forcing from the mean wind stress (of 0.0472 Pa toward 121.4° clockwise from true north), and an applied nudging boundary condition at the surface (with a nudging coefficient of 2.3×10^{-5} m s^{-1}) for the evolving (prognostic) baroclinic field—referenced to the climatological surface density. At the open boundaries the low-frequency and the M_2 forcings are specified, and the vertical structure of density is fixed at the climatological conditions (see Naimie, 1996).

With this set of initial and boundary conditions, the circulation is allowed to evolve, from an initial diagnostic condition (Naimie *et al.*, 1994), for eight M_2 periods (just over 4 days) and approach a dynamically consistent solution between the density, velocity and turbulent fields. Over these timescales, model solutions are not significantly different from solutions computed with the nudging coefficient set to zero. The model spatial resolution is variable, with grid size on the order of 500 m on the edges of the northern and southern flanks. The model time step was approximately 45 s. The depth-averaged flow field is shown in Fig. 2 and shows the familiar clockwise pattern around Georges Bank, including the tidally rectified northern flank jet, the southwestward drift along the southern flank and the generally weak recirculation in the Great South Channel during this season. The rate of dissipation of turbulent kinetic energy is presented in the Results section of this paper.

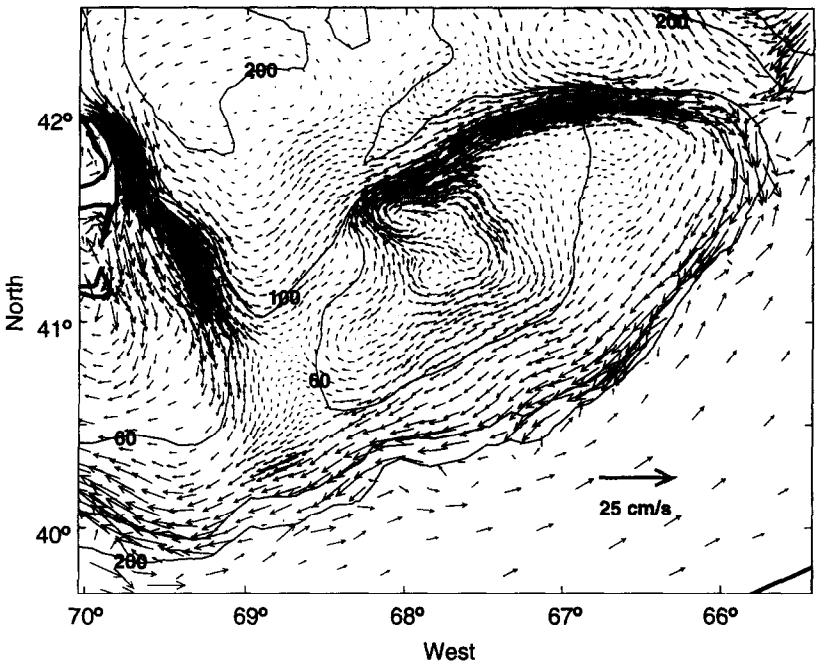

Fig. 2. Depth-averaged residual flow field.

Naimie (1996) has compared the diagnostic solution (Naimie *et al.*, 1994) and the prognostic solution described above. The cross-bank velocities are not significantly different from each other in the shallow regions on the Bank's crest. In deeper waters, the prognostic simulation predicts larger cross-bank velocities and a thinner surface Ekman layer due to the differences in the turbulence closure schemes used in the two studies. The two solutions are also in close agreement with observed flows along the northern flank, southern flank and Great South Channel regions (Naimie, 1996). In the Northeast Peak region, the "around-bank" residual transport stream-function of the prognostic solution shows roughly a 10% decrease compared to the diagnostic solution (Naimie *et al.*, 1994). The effect of the reduced transport in the Northeast Peak region on larval (particle) trajectories is a longer transit time from the Northeast Peak spawning grounds to the southern flank (Fig. 3), and thus, increased on-bank retention compared to the earlier study of Werner *et al.* (1993).

In the present study, during the last M_2 period of the simulation, we decomposed velocities and relevant turbulent quantities into a zero-frequency (residual or mean) component, and components at the M_2, M_4 and M_6 frequencies. For purposes of larval advection (i.e. particle tracking) and trophodynamic calculations we retained only the residual, the M_2 and M_4 components of velocity and turbulent dissipation, with those at the M_6 frequency found not to significantly affect our results. The effect of the wind is included in the mean circulation and turbulence components.

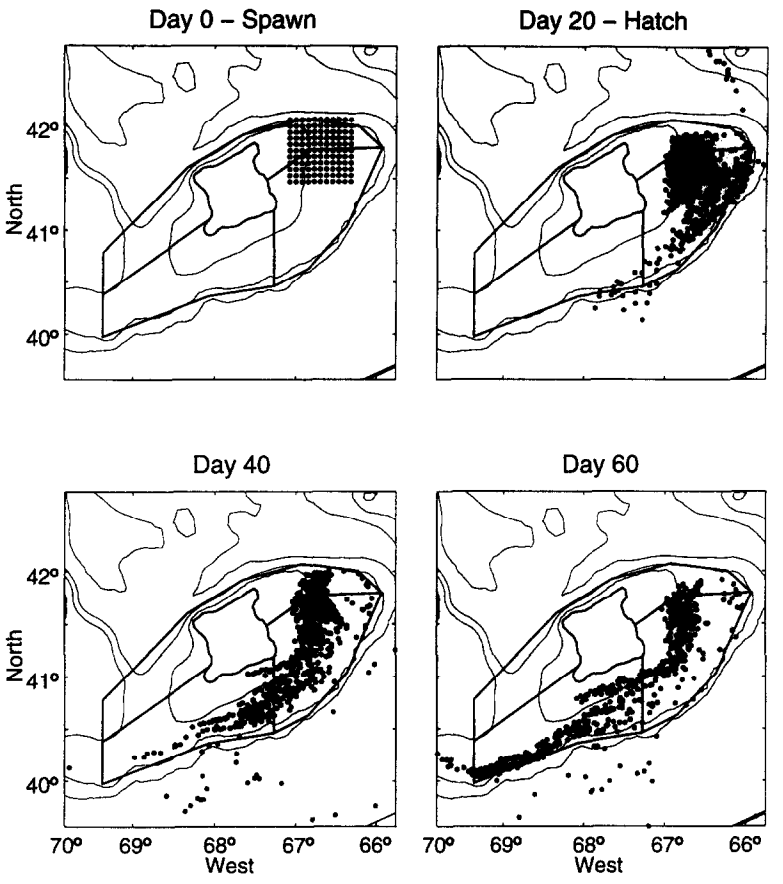

Fig. 3. Particle locations on Georges Bank at spawn (day 0), at hatch (day 20 post-spawn), 40 days post-spawn, and 60 days post-spawn; the particles were fully passive. Isobaths and regions as in Fig. 1.

4. TROPHODYNAMIC MODEL

The core of our model is the standard bioenergetic supply–demand function, in which growth is represented as the difference between the amount of food absorbed by a larva and the metabolic costs of its daily activities. Beyer and Laurence (1980) and Beyer and Laurence (1981) used this approach in individual-based models of winter flounder and Atlantic herring larvae. The amount of food ingested is a function of such processes as the number of prey encountered, captured and eaten, while the metabolic costs are a function of larval size, ambient temperature, swimming speed, etc. Larvae are assumed to die (of starvation) if their weight falls below a prescribed "death barrier". Using relationships derived from laboratory studies on the physiology and growth of Atlantic cod and haddock eggs and larvae, Laurence (1985) presented a model that included individual variation in hatch-size, prey density, prey size, and prey encounter rate. Our trophodynamic model is an elaboration of Laurence's (1985) model. In Laurence's formulation, ingestion of a single preferred prey size is modeled. In our model, the prey biomass ingested by the larvae is a

combination of the eight specified prey categories, with proportions of the ingested prey categories determined by Kane's (1984) analysis of the gut contents of particular size categories of cod and haddock larvae.

The application of our model can be viewed as having three components, each of which are sources of variability to the growth of individual larvae.

1. *Deterministic component*: in which larval feeding and growth are completely determined by empirical (laboratory-derived) relationships. In this case, the growth of a larva depends solely on its individual space–time trajectory through the fixed but spatially heterogeneous prey field;
2. *Stochastic component*: in which the additional effect of variability due to randomness in prey encounter and ingestion rate is imposed on individual larvae; and,
3. *Turbulent component*: in which the spatial and temporal variability of the encounters between larval predators and zooplankton prey is affected by the turbulence associated with the flow field.

4.1. *Deterministic component*

4.1.1. *Hatch.* Each larva (particle) is given a length at hatch. From Bolz and Lough (1988), the mean length of cod larvae (L_c) at hatch is 4.02 mm, with 95% confidence limits of 3.79–4.25 mm; the mean length at hatch for haddock larvae (L_h) is 3.32 mm, with the 95% confidence interval from 3.22 to 3.41 mm. In the present simulations, the hatch sizes of all larvae were assigned the mean lengths at age zero days from Bolz and Lough (1988), with no variation. Conversions to dry weight in μg for cod (w_c) and haddock (w_h) are

$$w_c = (L_c/1.935)^{(1/0.247)} \tag{1}$$

$$w_h = (L_h/2.026)^{(1/0.222)} \tag{2}$$

following Laurence (1985).

4.1.2. *Metabolic costs.* Given $w_{c,h}$, the metabolic cost is estimated in μg day^{-1} for cod and haddock

$$m_c = 24(0.010 \cdot w_c^{0.775}) \tag{3}$$

$$m_h = 24(0.038 \cdot w_h^{0.684}) \tag{4}$$

from Laurence (1978, 1985).

4.1.3. *Feeding.* We have ignored the 2–4 day yolk-sac stage and assumed that the larvae begin to feed at hatch. On any day the prey available for each larva depends on its location (see Fig. 1 and Table 1). The total prey biomass ingested by a larva is a combination of the eight specified prey categories, with proportions of the ingested prey items reflecting the ambient prey concentration and Kane's (1984) analysis of the gut contents of cod and haddock larvae as a function of larval size (see Tables 2 and 3).

An estimate of the number of the ith prey category $N(i)$ ($i = 1,2,\ldots, 8$) encountered over a 24-h period is obtained by accumulating all ith prey encountered at concentration $p_{c,h}(i)$ (no. l^{-1}) within each Δt time step

Table 2. Fractionation of preferred prey size of larval cod (ϕ_c) as a function of larval length L_c *(in* mm*) based on Kane's (*1984*) cod stomach content analysis. Refer to Table 1 for prey lengths and weights*

Prey type	$L_c < 5$ ϕ_c	$5 \le L_c < 6$ ϕ_c	$6 \le L_c < 7$ ϕ_c	$7 \le L_c$ ϕ_c
Eggs	0.23	0.2075	0.1725	0.1025
Nauplii	0.23	0.2075	0.1725	0.1025
C-I	0.23	0.2075	0.1725	0.1025
C-II	0.23	0.2075	0.1725	0.1025
C-III	0.01333	0.01667	0.03667	0.03667
C-IV	0.01333	0.01667	0.03667	0.03667
C-V	0.01333	0.01667	0.03667	0.03667
C-VI	0.04	0.12	0.20	0.48

$$N_{c,h}(i) = \sum_{24h} s_{c,h}^{\Delta t} \cdot \mathcal{L} \cdot p_{c,h}(i) \cdot \Delta t \tag{5}$$

where the search capacity per time step $s_{c,h}^{\Delta t}$ (liters/Δt) of the cod or haddock larva is obtained from the estimated daily search capacity $s_{c,h}$ (l day^{-1}) given by Laurence (1985)

$$s_c = 0.737 w_c^{0.741} \tag{6}$$

$$s_h = 0.846 w_h^{0.666} \tag{7}$$

and $\mathcal{L}$ is a day/night binary switch which is unity during daylight hours and zero at night. The fraction of daylight hours is a function of latitude and day of the year and is computed from Morse (1989).

The prey biomass $P_{c,h}$ ingested by a cod or haddock larva is the sum of the number of prey items encountered $N_{c,h}(i)$, each scaled by the fraction of the particular prey type $\phi_{c,h}(i)$ found in the gut of that larval size class for cod or haddock (Tables 2 and 3)

$$P_{c,h} = \sum_{i=1}^{8} [s1_{c,h} \cdot \phi_{c,h}(i) \cdot N_{c,h}(i) \cdot w_p(i)] \tag{8}$$

Table 3. Fractionation of preferred prey size of larval haddock (ϕ_h) as a function of larval length L_h *(in* mm*) based on Kane's (*1984*) cod stomach content analysis. Refer to Table 1 for prey lengths and weights*

Prey type	$L_h < 5$ ϕ_h	$5 \le L_h < 6$ ϕ_h	$6 \le L_h < 7$ ϕ_h	$7 \le L_h$ ϕ_h
Eggs	0.23	0.235	0.205	0.145
Nauplii	0.23	0.235	0.205	0.145
C-I	0.23	0.235	0.205	0.145
C-II	0.23	0.235	0.205	0.145
C-III	0.02333	0.01333	0.02	0.02667
C-IV	0.02333	0.01333	0.02	0.02667
C-V	0.02333	0.01333	0.02	0.02667
C-VI	0.01	0.02	0.12	0.32

where $w_p(i)$ is the dry weight (μg) of the ith prey category and $sl_{c,h}$ is the swallowing probability of cod and haddock larvae

$$sl_c = 0.9\left[1 - 0.667e^{-0.0040(w_c - w_c^{min})}\right] \tag{9}$$

$$sl_h = 0.9\left[1 - 0.778e^{-0.0045(w_h - w_h^{min})}\right] \tag{10}$$

determined empirically (Laurence, 1985) where $w_{c,h}^{min}$ is the initial (minimal) dry weight at hatch (μg) of the cod or haddock larva (taken from Bolz and Lough, 1988).

4.1.4. *Growth.* The daily larval growth increment $G_{c,h}$ is determined as the difference between the weight gained through feeding ($g_{c,h}$) and the weight lost due to metabolic costs ($m_{c,h}$)

$$G_{c,h} = g_{c,h} - m_{c,h} \tag{11}$$

where $m_{c,h}$ is defined above, and

$$g_{c,h} = (1 - \alpha) \cdot \beta_{c,h} \cdot P_{c,h} \tag{12}$$

in which α ($=0.4$) is the cost of processing and utilizing the digested food, and

$$\beta_{c,h} = 0.8[1 - 0.625e^{-0.002(w_{c,h} - w_{c,h}^{min})}] \tag{13}$$

is the fraction of food ingested that is actually digested by the larva (Beyer and Laurence, 1981).

We limit maximum growth (determined by $G_{c,h}$) to 15% of larval body weight per day to account for satiation of feeding, and maximum weight loss to (minus) 10% body weight per day to account for utilization of body energy reserves (Laurence, 1985). Once $G_{c,h}$ is known the new weight of the cod or haddock larva is obtained from

$$w_{c,h}^{new} = w_{c,h} + G_{c,h} \tag{14}$$

in μg dry weight.

4.1.5. *Death.* Finally, a minimum, or death, size (μg dry weight) is prescribed for each cod and haddock larva, based on the minimum size of live larvae that occurred in experiments at the Narragansett laboratory and the assumption that larvae smaller than this size had died (Laurence, 1985)

$$w_c^b = w_c^{min} e^{0.0282T} \tag{15}$$

$$w_h^b = w_h^{min} e^{0.0226T} \tag{16}$$

where T is the age of the larva in days. If the weight of a larva falls below $w_{c,h}^b$ on any given day, the larva is judged to be dead.

4.2. *Stochastic component*

Stochastic, or probabilistic, approaches allow the parameterization of random processes that otherwise cannot be explicitly included in a model formulation. We considered two stochastic components to the deterministic formulation: the number of prey encountered

and the number of prey ingested (see also Beyer and Laurence, 1980) on a daily basis. Random variations in the number of prey encountered were simulated assuming a negative binomial distribution (e.g. Owen, 1989; Winemiller and Rose, 1993). Given the deterministic number of prey encountered in each prey category $N_{c,h}(i)$, a random deviate was chosen (per prey category) from a negative binomial distribution subject to a contagion parameter, e.g. $K = 1$ to simulate patchiness or $K = 10$ for a more uniform (Poisson-like) distribution. The number of prey captured and ingested by an individual cod or haddock larva is obtained as a random deviate from a binomial distribution (Beyer and Laurence, 1980) given the number of prey encountered per prey category and given the swallowing probability, or probability of capture, $sl_{c,h}$. Additional stochastic components, such as the size distribution at hatch, undoubtedly play a role and are straightforward additions in the above formulation, but have not been included in the present study.

4.3. *The effect of turbulence on encounter rates*

Rothschild and Osborn (1988) discussed the role of turbulence in affecting (enhancing) encounter rates with planktonic prey. Subsequent studies, e.g. Sundby and Fossum (1990), MacKenzie and Leggett (1991) and Muelbert *et al.* (1994), explored the role of turbulence in oceanic conditions, finding an effective increase in contact rates of 2–10 under various wind- and tidally-driven flows. To estimate the number of prey encountered over a 24-h period in a turbulent environment, we use

$$N(i) = \sum_{24h} \mathcal{L} \cdot A(i) \cdot D \cdot p(i) \cdot \Delta t \tag{17}$$

instead of Equation (5). The effect of the turbulent velocity ω enters in the determination of $A(i)$, the velocity of a larval fish relative to its prey.

$$A(i) = \frac{[\sigma^2(i) + 3\tau^2 + 4\omega^2]}{3(\tau^2 + \omega^2)^{1/2}} \tag{18}$$

where the larval fish swimming speed τ, and the ith prey swimming speed $\sigma(i)$ are assumed here as 1 body length per second. In Equation (17) $\mathcal{L}$ is as before, the binary day/night switch and D is the cross-sectional area of perception of the larva

$$D = \frac{2}{3}\pi\rho^2 \tag{19}$$

where ρ is the prey encounter radius which is related to the larval cod or haddock body length (Laurence, 1978)

$$\rho = \frac{3}{4}L_{c,h} \tag{20}$$

and $p(i)$ is as before, the concentration of the ith prey item. The turbulent velocity (squared) is

$$\omega^2 = 3.615(\varepsilon r)^{2/3} \tag{21}$$

where the separation distance can be approximated (Rothschild, 1992) as

$$r = 0.55p(i)^{-1/3} \tag{22}$$

and ε is the rate of turbulent kinetic energy dissipation

$$\varepsilon = \frac{q^3}{B_1 l} \tag{23}$$

which is obtained at every point in space and time throughout the model domain. The turbulent velocity, q, and the mixing length, l, are obtained from the circulation model and $B_1 (= 16.6)$ is a constant (Mellor and Yamada, 1982; Galperin *et al.*, 1988).

In the cases where the turbulence-enhanced contact rates are used, once the number of prey encountered $N(i)$ is determined using Equation (17) [rather than Equation (5)], the computation of total prey biomass, feeding, growth, etc., continues as before from Equation (8) to Equation (16). For the turbulence affected cases shown herein, the number of prey encountered and the number ingested was randomized as described in Section 4.2, with the contagion parameter (K) set to 10. A time step Δt of 1 h was used in all trophodynamic calculations.

5. RESULTS

The circulation is used to derive trajectories for the transport of larvae and their location each hour determines the amount of food available based on the ambient prey concentration. Spawning is assumed to occur on the Northeast Peak, and the larvae drift passively with the circulation. Particles were released over the Northeast Peak at 1, 10, 20, 30, 40 and 50 m in a square region 62.5 km on a side (Fig. 1). At each horizontal level there were 121 particles equally spaced in an 11×11 grid, resulting in a total of 726 particles per release. The egg-phase is assumed to be 20 days long (Page and Frank, 1989). At 20 days post-spawn the larvae hatch and trophodynamic processes (feeding, growth, starvation) begin. We consider trophodynamics only for the first 40 days of the larval period for a total length of the simulations of 60 days: a 20-day egg-phase and a 40-day larval-phase.

First we consider the baseline case where losses are due only to advective processes, i.e. no starvation. The location of the particles at hatch (20 days post-spawn), at 20 days post-hatch and at 40-days post-hatch is shown in Figure (3). These results are consistent with those described in Werner *et al.* (1993) and Lough *et al.* (1994) wherein those larvae in the top 20–25 m, or seaward of the 70 m isobath, are lost from the Bank while those below 25 m or shoalward of the 70 m isobath are more likely to be retained on the Bank. In the case considered herein we have not included the effect of behavior, e.g. vertical migration (Lough and Potter, 1993). Defining "on-Bank" as locations shallower than 100 m and east of 69°W (east of the Great South Channel), a 10% loss off-Bank already is observed at hatch (i.e. during the 20-day egg-phase), followed by a roughly monotonic increase in off-Bank losses of larvae to the Gulf of Maine, deep ocean and to the Middle Atlantic Bight over the next 40-days, with approximately 15% of the total number of larvae spawned on the Bank lost by day 60 post-spawn (Fig. 4). The small increase in the number of on-Bank larvae during the first 5 days post-hatch is a result of the recirculation features along the Bank's edge along northern and eastern flank regions.

We next examine trophodynamic effects. All larvae at hatch are assigned to be of equal size. Variability in their (daily) growth is introduced by the spatially heterogeneous distribution of prey, the stochastic variations about the number of prey encountered and ingested, and finally, by the three-dimensional distribution of turbulence as it affects larval fish–prey encounter rates. The hourly position of each larva is used to determine its growth,

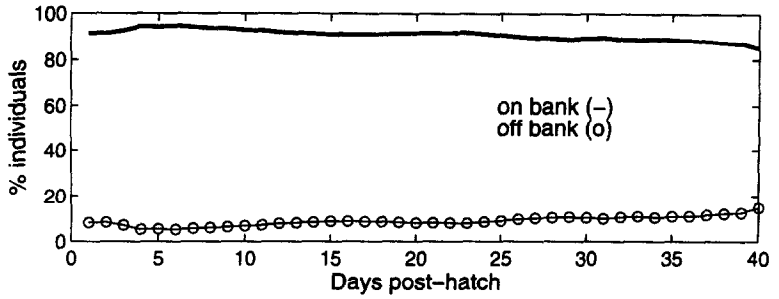

Fig. 4. Effect of advection on the post-hatch time history of cod larvae on-Bank (solid line) and off-Bank (solid line with open circles). At hatch, 10% of the eggs spawned on the Bank have been lost off-Bank; at day 40 post-hatch there is an additional 5% loss of larvae, resulting in a total loss due to advection of approximately 15%.

i.e. every hour an estimate is made of each larva's location, the amount of food it ingested and the turbulence field in which it is located. We first present the results of the simplest (deterministic) formulation, then we present effects of the inclusion of the turbulence field on the encounter rate between prey and larva (including probabilistic elements).

5.1. *Deterministic prey encounter and ingestion*

In the deterministic case, the specified distribution and abundance of prey is insufficient for the survival and growth of cod and haddock larvae. Both cod and haddock larvae starve by 2–3 days post-hatch (Fig. 5). The 2–3 day survival of the larvae at this food concentration arises from the difference in the initial weight of the larvae at hatch (the mean value observed by Bolz and Lough, 1988) and the smallest size observed at hatch (also from Bolz and Lough, 1988)—where the latter value was used to estimate the death barrier ($w^b_{c,h}$). Thus, it takes 2–3 days for the larvae that hatched at the mean observed size to reach the limiting death barrier.

The effect of increasing 5-fold the concentration of the four smallest prey items (eggs, nauplii, and copepodite stages C-I and C-II) encountered by cod larvae is shown in Fig. 6. Haddock larvae required a 15-fold increase in these concentrations to achieve similar results (Fig. 7). At the end of 40 days post-hatch, the fraction of larvae starved on the Bank was roughly 15% for cod and 45% for haddock, with advective losses in each case of about 12–15%. Note that these percentages are all relative to the total number of eggs spawned, i.e.

Fig. 5. Post-hatch time history of cod larvae in the deterministic case showing the percentage of larvae alive (solid line), starved on-Bank (solid line with crosses), and advected off the Bank (solid line with open circles).

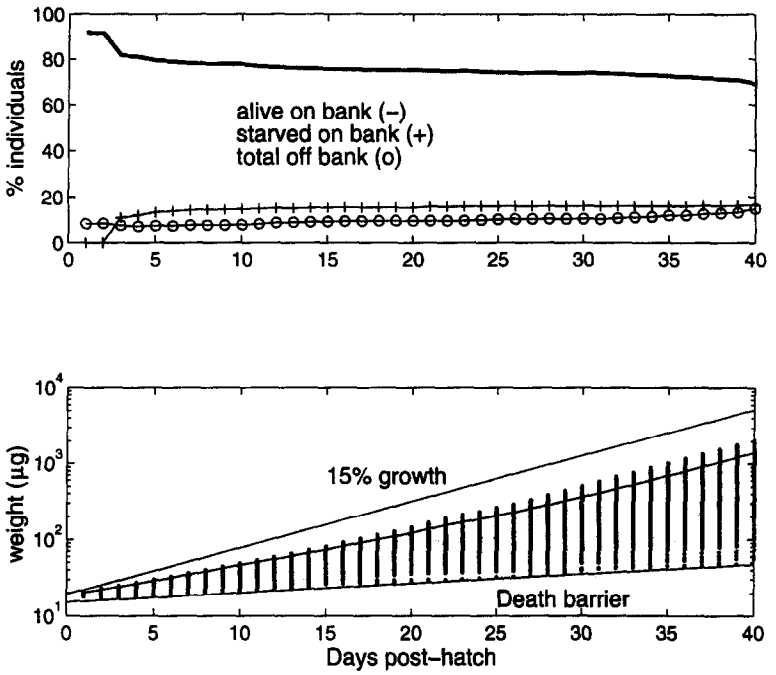

Fig. 6. Post-hatch time history of cod larvae in the deterministic case with a 5-fold increase of egg, nauplii, C-I and C-II prey categories showing, in the upper panel, the percentage of larvae alive (solid line), starved on-Bank (solid line with crosses), and advected off the Bank (solid line with open circles); and, in the lower panel, the daily size distribution (μg) for the live larvae on the Bank. Also indicated in the lower panel is the 15% per day growth curve, the death barrier and the mean weight of those live larvae still on the Bank.

the initial 726 particles released. The result is that 70% of the cod and 40% of the haddock larvae remain alive and on-Bank after 40 days post-hatch. Mean growth rates (in weight) of up to 10% per day for those larvae on the Bank were as observed for cod and haddock on Georges Bank over the first two months by Bolz and Lough (1988). Leaving the concentrations of the four smallest prey items as originally specified and increasing the concentration of the four largest prey items caused all larvae to die within 2–3 days post-hatch, illustrating the sensitivity of larval fish to prey availability at first feeding (because of their proximity to the "death barrier").

The trajectories and the amount of time spent in the various regions by the surviving larvae is critical in determining growth rates and larval sizes to day 40. For example, the resulting size distribution of cod larvae at day 40 for the simulation of Fig. 6 is shown in Fig. 8. The observed size distribution arises from the differing amounts of time spent by the larvae in the eastern and southern flank regions. The largest larvae (corresponding to those > 1800 μg in Fig. 8; also Fig. 9) are those that spent the longest time in the eastern flank region, which was assigned to have a high proportion of small prey. Larva no. 719 (Fig. 9) spends all but the last few days in the EF region and grows to over 13 mm in length. By contrast, larva no. 460, initially in the EF, is advected into the SF region on day 22, at which time its growth rate decreases, reaching a length of roughly 11 mm after 40 days. Even brief excursions from the EF region to neighboring regions during the early stages of larval

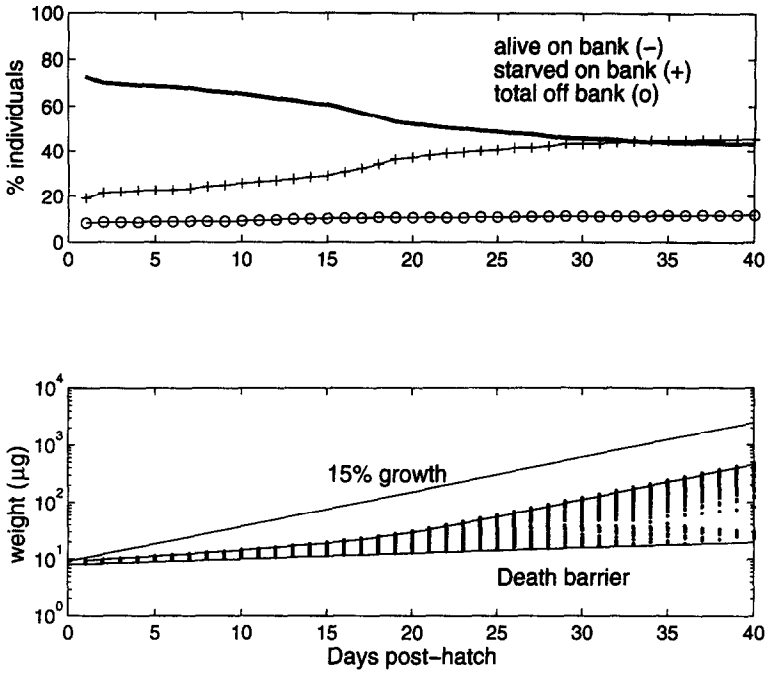

Fig. 7. Post-hatch time history of haddock larvae in the deterministic case with a 15-fold increase of egg, nauplii, C-I and C-II prey categories showing, in the upper panel, the percentage of larvae alive (solid line), starved on-Bank (solid line with crosses), and advected off the Bank (solid line with open circles); and, in the lower panel, the daily size distribution (μg) for the live larvae on the Bank. Also indicated in the lower panel is the 15% per day growth curve, the death barrier and the mean weight of those live larvae still on the Bank.

growth can have a significant impact on the size of the later stages. Specifically, tidal currents advect larva no. 3 between the NF region and the EF region during the first 6 days post-hatch. The difference in growth rates and resulting size for larva no. 3 during these 6 days and the sizes of either larva no. 719 or no. 460, is clear. Finally, larva no. 595 spends all but the first 6 days in the SF region. While it does not starve, larva no. 595 grows very slowly during the 34 days it spends in the SF region. A quick exit from the EF region exposes small

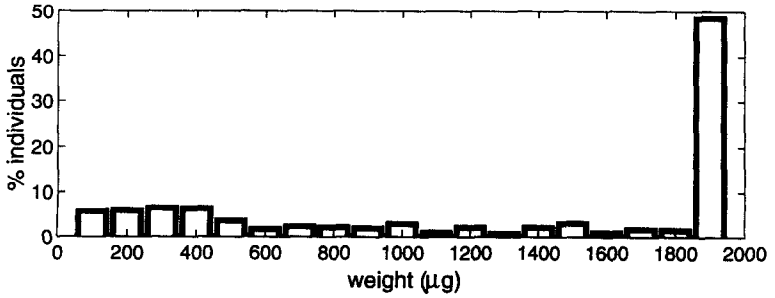

Fig. 8. Weight distribution (μg) at day 40 for live cod larvae on the Bank in the deterministic case with a 5-fold increase of egg, nauplii, C-I and C-II prey categories (see Fig. 6).

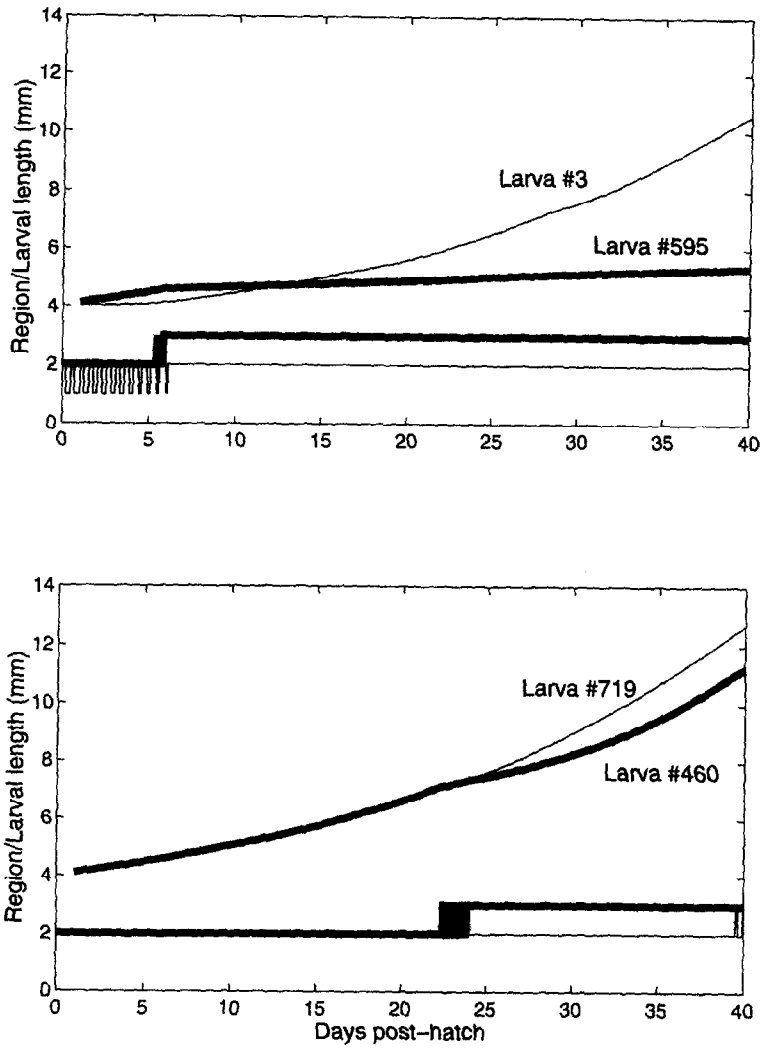

Fig. 9. Growth time-histories for selected larvae (nos 3, 460, 595 and 719) under the deterministic case with a 5-fold increase of egg, nauplii, C-I and C-II prey categories. The ordinate axis indicates both the larval length (upper two curves in each panel) and the region in which a larva—identified by either the thin or thick line—is located (lower two curves in each panel), with the (NF, EF, SF and CC) regions (Fig. 1) being regions (1,2,3,4), respectively.

larvae to a prey size distribution (dominated by large prey categories) that is generally too large for them to consume.

5.2. *Random prey encounter and ingestion*

Randomizing the number of prey encountered and ingested by cod larvae about their expected (mean) values simulates the encounter by some larvae of higher (or lower) prey

densities and greater (or reduced) success at capturing and ingesting prey. Using the prey densities prescribed in Table 1, we were not able to generate cases where larvae would survive the entire 40 days of the simulation through "random" chance; at best, the lifetime of certain larvae was lengthened to 6–7 days (compared to 3 days in Fig. 5). The need for a 5-fold increase in prey concentration for survival of cod (Fig. 6), and 15-fold for haddock (Fig. 7) indicates that large increases of prey relative to the (prescribed) mean are necessary. In the case of stochastic simulations, the negative binomial distribution with a small contagion parameter may generate a sequence of deviates that could simulate the encounter of a larva with a high concentration patch, or patches, of prey. However, the small number of larvae considered in our simulation is not likely to be an adequate sample size. Other extensions to stochastic approaches should include the ability of larvae to alter their behavior (e.g. forage) in the patch, perhaps by considering the encounter with a patch as a Markovian process. Similarly, the specification of the contagion parameter as a function of local turbulence intensity could also be explored. We do not consider these extensions in the discussions that follow, focusing instead on the effect of turbulence on the encounters between larvae and prey.

5.3. *Effects of turbulence on encounter rates*

The rate of turbulent kinetic energy dissipation ε for the March–April flow field used in our study is shown in Figs 10 and 11. The ε fields include contributions from the mean (zero-frequency), M_2 and M_4 frequencies. In the horizontal plane inside the 60 m isobath (Fig. 10), the depth-averaged dissipation rate $\bar{\varepsilon}$ is greatest on the Bank crest reaching values as high as $10^{-5}\,\mathrm{W\,kg^{-1}}$ and never below $10^{-6}\,\mathrm{W\,kg^{-1}}$. At the southern edge of the Bank, $\bar{\varepsilon}$ drops to $10^{-7}\,\mathrm{W\,kg^{-1}}$. A vertical section across the northern and southern flanks (Fig. 11) shows ε values as high as $10^{-4}\,\mathrm{W\,kg^{-1}}$ near the bottom over the Bank crest and values generally greater than $10^{-6}\,\mathrm{W\,kg^{-1}}$ within the (roughly 25 m thick) bottom tidal boundary layer. Near the surface, where effects of wind are largest, the turbulent dissipation rates are between 10^{-7} and $10^{-6}\,\mathrm{W\,kg^{-1}}$. These values are in good agreement with the values observed by Loder *et al.* (1993) and Horne *et al.* (1996) over the bank crest and the northern flank, and those inferred by Incze *et al.* (1996) and Lough and Mountain (1996) on the southern flank.

Vertical profiles of ε during two tidal cycles at three stations on the southern flank (Fig. 12) show the bottom and surface intensified values of dissipation due to tidally- and wind-induced shears, with the near bottom values always greater than the surface values. Similarly, the absolute magnitude of ε is highest at the shallow station (Site III) and smallest at the deepest station (Site I; see also Fig. 11). The vertical profile of the density at the three sites is shown in Fig. 13, with the shallowest station (Site III) being well-mixed (showing practically no vertical stratification), and the deepest (Site II) indicating the presence of a pycnocline between 15 and 30 m depth. [Note that the absolute strength of the stratification is greatest at the offshore site (Site II) where the range of σ_t values is between 26.70 and 26.90, weakest at the shallow station (Site III) where the values of range σ_t is of 26.75 ± 0.05, and with Site I being representative of intermediate conditions (Fig. 13).] With the values of ε shown in Fig. 12 and the prey (e.g. nauplii) concentrations of Table 1 for the southern flank region, contact rates between larvae and nauplii at these stations can be obtained from Equation (17). For example, choosing larval and naupliar swimming speeds of $5.5\,\mathrm{mm\,s^{-1}}$ and $0.55\,\mathrm{mm\,s^{-1}}$, respectively, time-history profiles during two tidal cycles of absolute

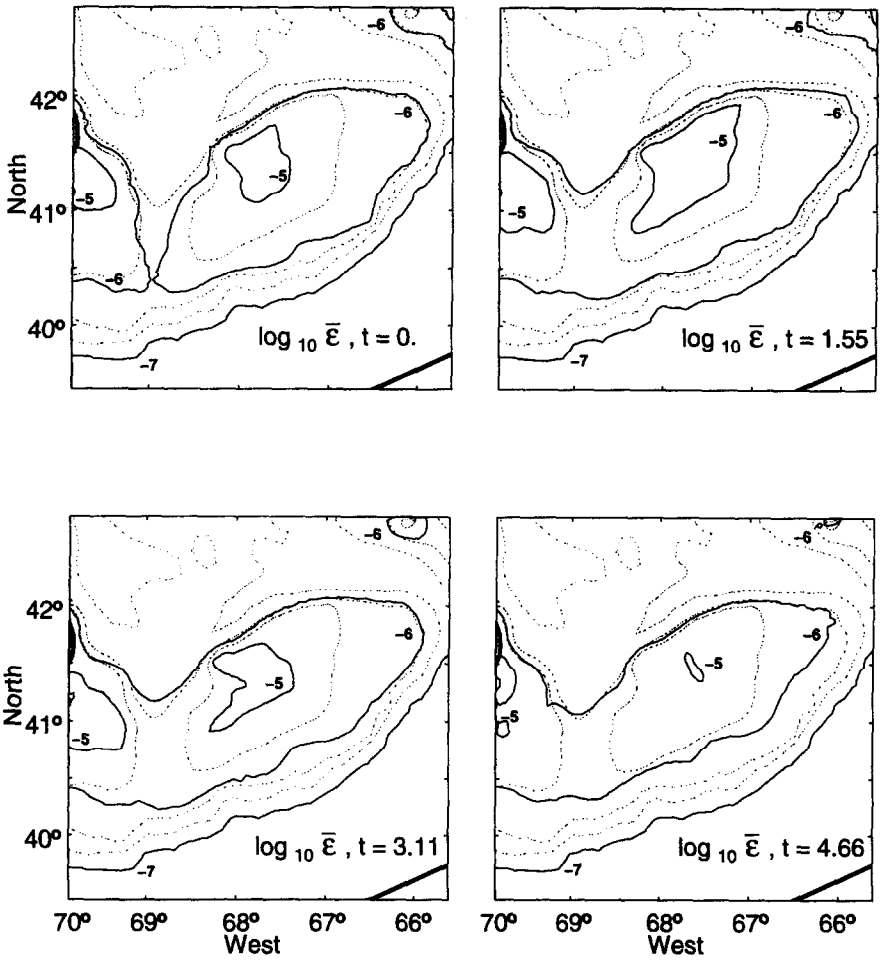

Fig. 10. Depth-averaged turbulent kinetic energy dissipation rate $\bar{\varepsilon}$ (W kg^{-1}) sampled at four times during an M_2 tidal cycle. Time (t) is in hours; isobaths (dotted lines) as in Fig. 1.

contact rates are shown in Fig. 14. Relative increases in contact rates (Fig. 15) show 2–5-fold increases when turbulence is included compared with the "no-turbulence" case, i.e. when the turbulent velocity ω is zero. Note that since the prey field was specified as vertically uniform, the vertical structure in contact rates is provided entirely by the vertical structure in the turbulent kinetic energy dissipation rate, with increased values of ε near the wind-driven surface layer and the tidal bottom boundary layer.

The effect of the turbulence-enhanced contact rates on the growth and survival of cod is shown in Fig. 16. With the concentration of prey as in Table 1, there is high initial mortality but some cod larvae survive for the entire 40-day period. In addition, the size distribution is broad with some larvae growing at the observed rates (Bolz and Lough, 1988) of 10% per day in weight. These results contrast with the deterministic case, in which no larvae survived

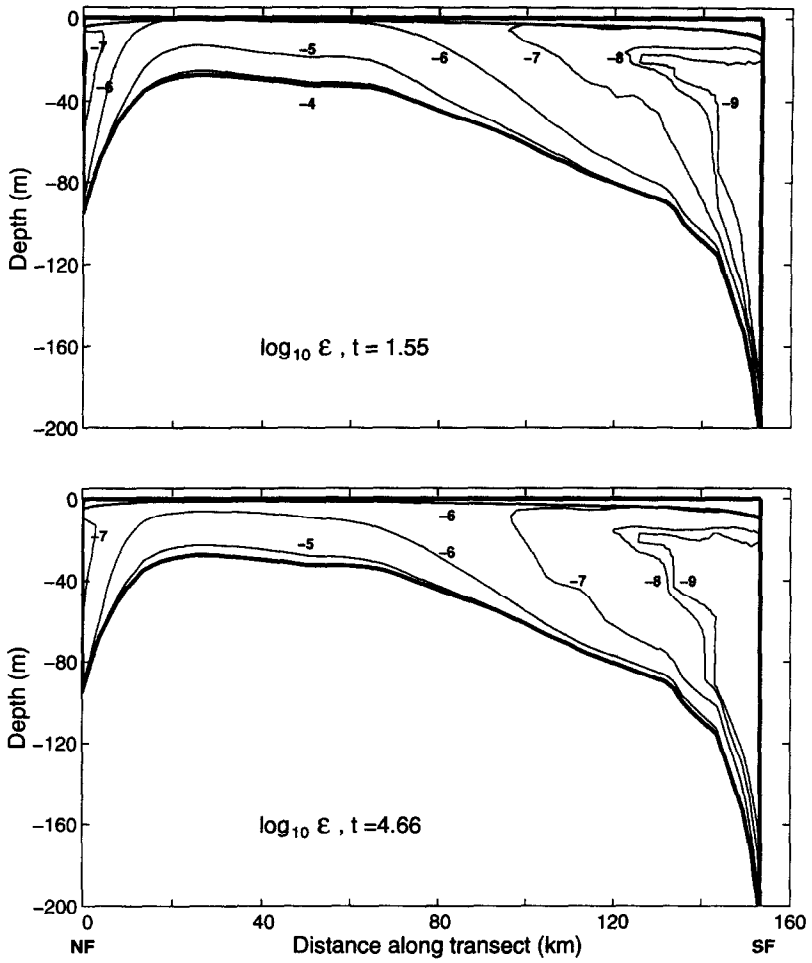

Fig. 11. Vertical section of turbulent kinetic energy dissipation rate ε (W kg^{-1}) across the Bank from northern (NF) to southern flank (SF), along the transect indicated in Fig. 1, for the t = 1.55 h and t = 4.66 h snapshots shown in Fig. 10.

more than 3 days (Fig. 5). Including effects of turbulence on contact rates, all surviving cod larvae straddled the 60 m isobath (Fig. 17), and were in the water column at depths greater than 25 m; the mean depth of the surviving larvae was 55 m. This is also the location on the Bank and the depth in the water column identified by Werner *et al.* (1993) and Lough *et al.* (1994) as the most retentive region on the Bank due to the circulation.

The results for haddock are similar to those for cod in that the increased encounter rate due to turbulence reduces the starvation mortality, but the prey concentrations (Table 1) still need to be increased by a factor of five before any larvae survive (Fig. 18). This is in contrast to the deterministic case, in which prey concentrations 15 times those initially specified were needed to get reasonable haddock survival and growth rates (e.g. Figure 7).

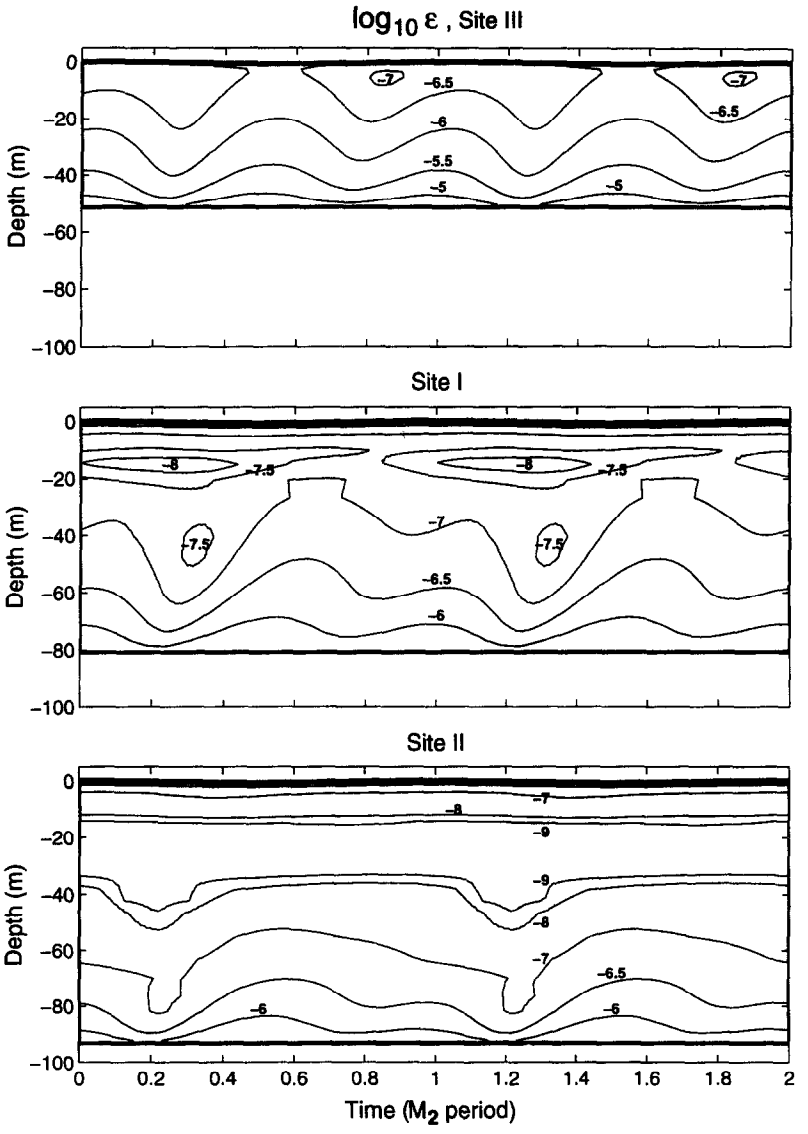

Fig. 12. Vertical profiles of the turbulent kinetic energy dissipation rate ε (W kg^{-1}) over two tidal cycles at Sites I, II and III on the southern flank (see Fig. 1). The time-series were reconstructed using the residual, M_2 and M_4 components.

6. DISCUSSION

The model results allow us to consider the relative effects of advective and trophodynamic processes on the retention, growth and survival of larval cod and haddock populations on Georges Bank during the late winter/early spring season. Specific conclusions that may be drawn are:

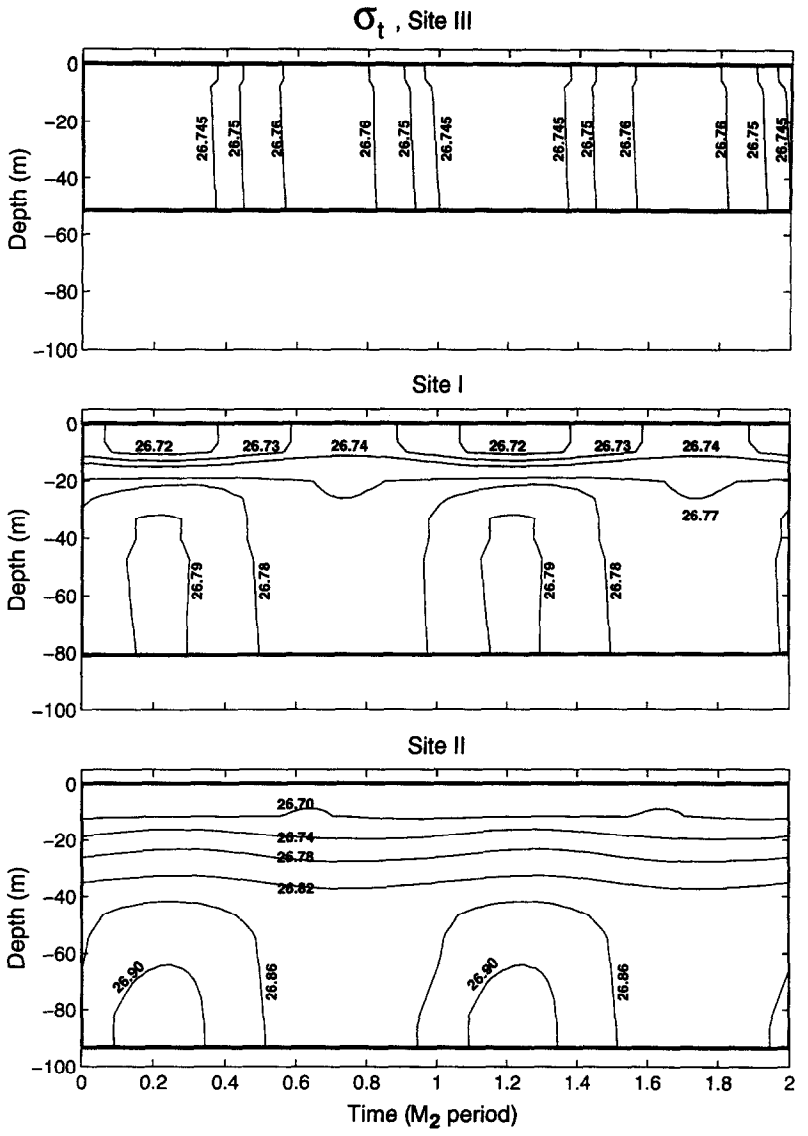

Fig. 13. Vertical profiles of density (σ_t) over two tidal cycles at Sites I, II and III on the southern flank (see Fig. 1). The time-series were reconstructed using the residual, M_2 and M_4 components.

1. Significant differences can arise in the starvation mortality and the growth rates of larvae on the Bank, and losses due to advection off the Bank, when individual variability is introduced in just two parameters: the number of prey encountered per day and the success at capturing and ingesting those prey.

2. Spatial variability in prey distributions can influence the growth rates and resulting size distributions of larvae in different regions of Georges Bank. Recently hatched larvae grew better the longer they persisted in the eastern flank region where the concentration of nauplii was greatest.

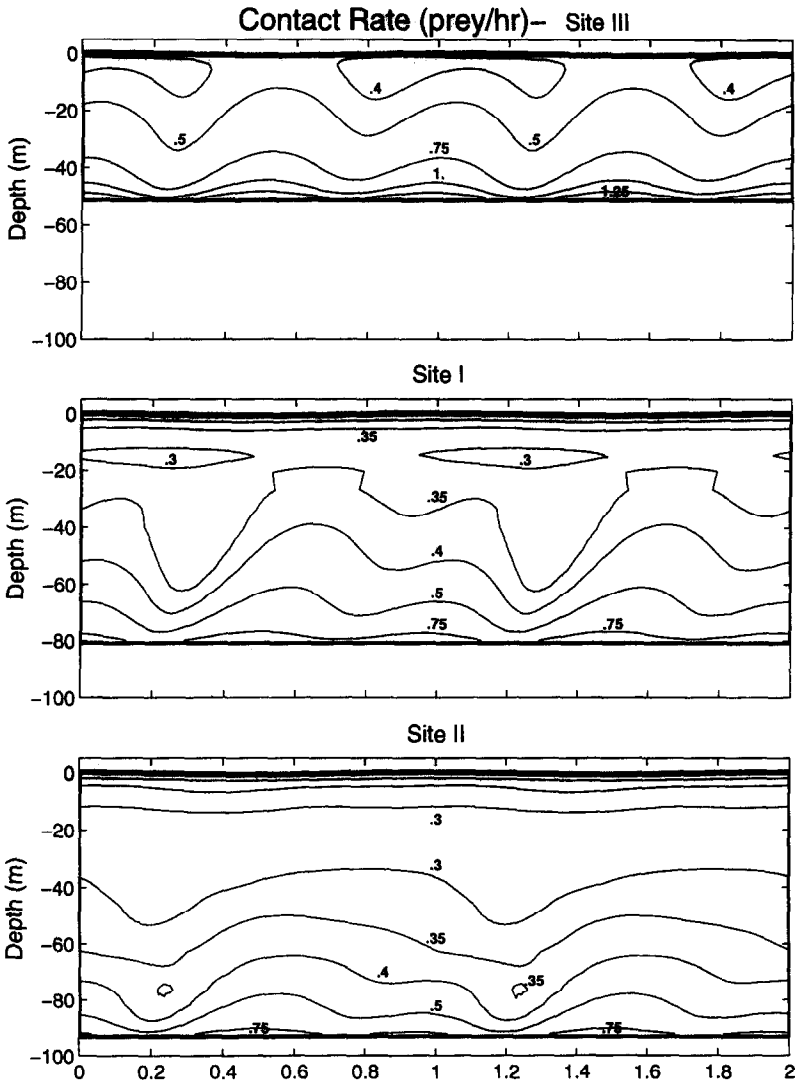

Fig. 14. Larval cod contact rates (prey per hour) during two tidal cycles at Sites I, II and III on the southern flank (see Fig. 1). The contact rate was computed using the values of ε shown in Fig. 12, for a larval length of 5.5 mm and prey lengths and concentrations corresponding to nauplii as in Table 1 for the southern flank.

3. Using estimates for early late winter/early spring *mean* prey fields, the model predicts that cod and haddock larvae will starve on Georges Bank. Five-fold increases in the mean prey concentrations were necessary for cod larvae to survive, while 15-fold increases were required for survival of haddock larvae.

4. Spatially-variable and time-dependent turbulence generated by winds and tides increases prey contact rates, effectively increasing the prey concentration perceived by the

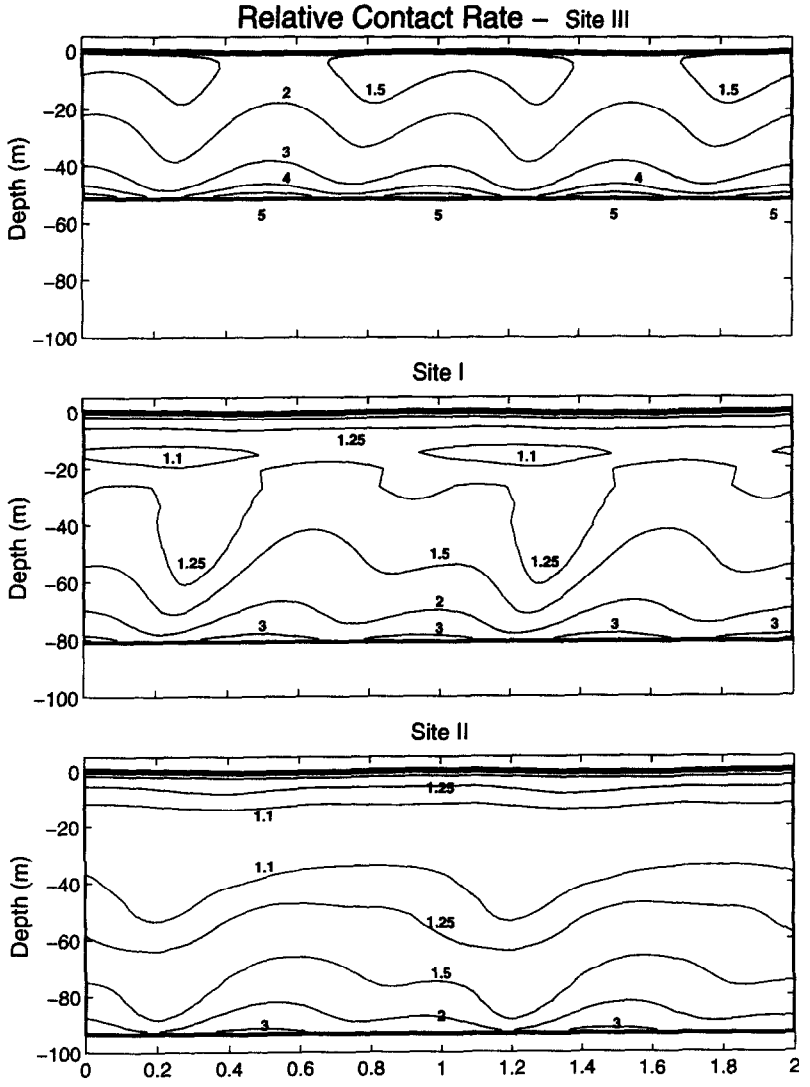

Fig. 15. Relative (dimensionless) contact rates (turbulence-enhanced/no turbulence) during two tidal cycles at Sites I, II and III (see Fig. 1) on the southern flank. The effect of turbulence (see Fig. 14) increases the larval–prey contact rates by a factor of 2–5 over the no-turbulence case.

larvae. The result is an increase in the larval growth and survival rates that are comparable with observed growth rates.

5. Effective increases in the contact rates due to turbulence are 2–5 times greater than the contact rates with no turbulence, in agreement with the required increases in prey concentrations (at least for cod) in the absence of the turbulence-enhanced larval–prey contact rates. Thus model cod larvae were able to survive and grow at observed rates with the imposed mean prey concentrations, while model haddock required an increase of a factor of 5 (compared to 15 in the absence of turbulence). Turbulence-enhanced contact

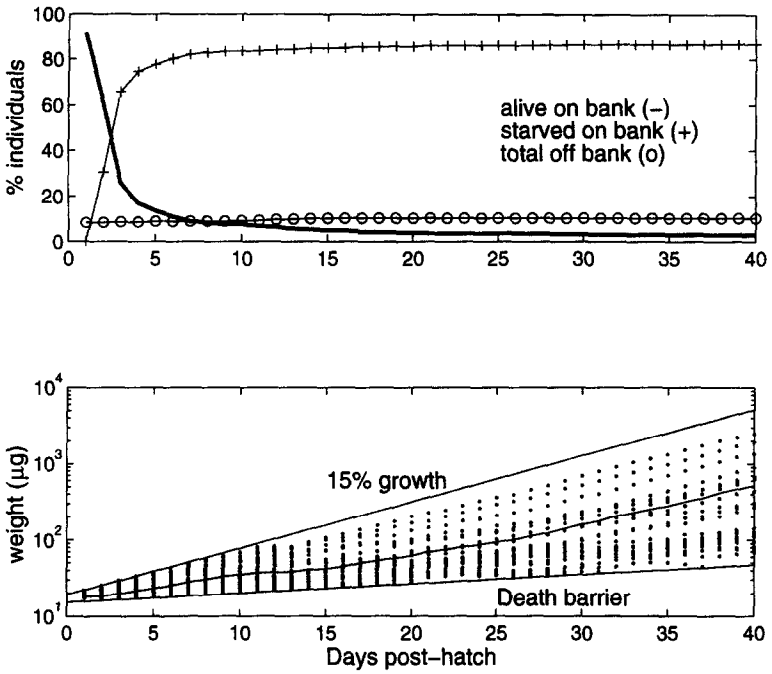

Fig. 16. Post-hatch time history of cod larvae including turbulence-enhanced contact rates showing, in the upper panel, the percentage of larvae alive (solid line), starved on-Bank (solid line with crosses), and advected off the Bank (solid line with open circles); and, in the lower panel, the daily size distribution (μg) for the live larvae on the Bank. Also indicated in the lower panel is the 15% per day growth curve, the death barrier and the mean weight of those live larvae still on the Bank.

rates are thus determined to be a necessary component in our description of the growth of cod and haddock larvae on Georges Bank.

6. Larvae with growth rates comparable to those observed in the field are located below the surface layer (deeper than 25 m) and inside the 60 m isobath. In the cases we considered, tidally-induced turbulence in the bottom boundary layer provides the required increases in prey contact rates. Thus, the region of highest retention due to circulation processes coincides with the region of highest growth rates: shoalward of the 60 m isobath, at subsurface depths of 25 m or greater.

7. Haddock larvae require higher prey densities than cod larvae to survive. This may be a result of the vertically uniform specification of the prey field in the present formulation (see below).

The divergence in larval size illustrates the advantages of remaining longer on the eastern flank, at least under the scenario that this region has higher concentrations of small prey. Larvae which grow quickly during the first few days post-hatch move away from the "death" size limit, and since search capacity and prey capture success are both functions of larval size, larger larvae encounter more prey and have greater success at their capture and ingestion. This suggests that the timing of spawning relative to the zooplankton production cycle, and in particular the distribution of early nauplius and copepodite stages, is as

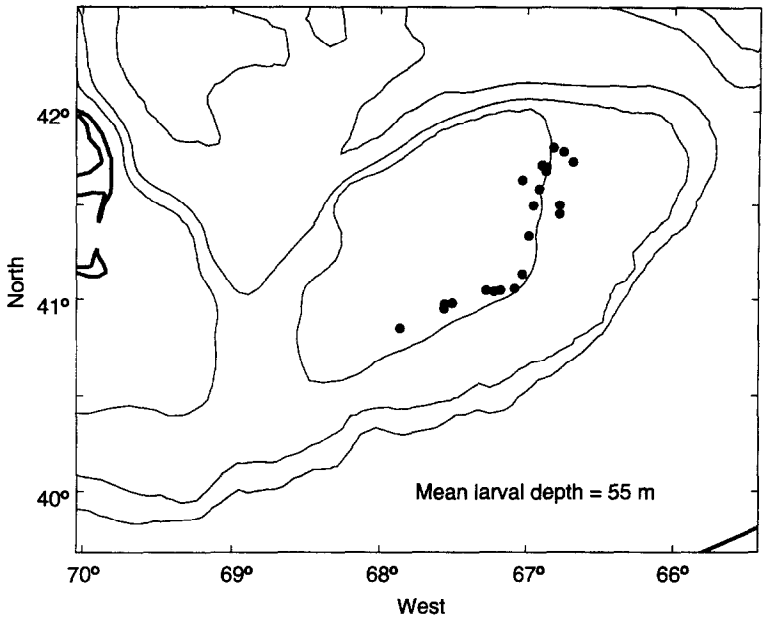

Fig. 17. Horizontal positions of the live cod larvae at day 40 post-hatch (day 60 post-spawn; see Fig. 3) including turbulence-enhanced contact rates. The mean depth of the live larvae is indicated. Isobaths as in Fig. 1.

important for Georges Bank as has been suggested for other areas (e.g. Brander and Hurley, 1992; Brander, 1994). The greatest effect of inadequate prey for larval cod and haddock on Georges Bank occurs during the first few days post-hatch, i.e. the beginning of exogenous feeding. If larvae survive this period, their probability of survival through at least the next 40 days is high, although growth rates and resulting sizes of larvae will depend on the concentrations of prey encountered. The importance of this first-feeding period has been clearly demonstrated for other fish larvae (e.g. Theilacker *et al.*, 1996). In addition to the timing match between larval fish development and prey distribution, interannual variability in the intensity of the circulation and its effectiveness at transporting larvae away from the eastern flank (e.g. caused by variations in wind and storm intensity; cf. Lough *et al.*, 1994) are also very important. In contrast, the predominance of tidally-generated turbulence suggests that at least cod populations may have evolved to depend on its presence. The requirement by haddock for higher prey concentrations, such as occur about fronts and pycnoclines which also have lower turbulent dissipation rates, may represent an important difference between the two gadid species.

With respect to Hjort's (1914) two hypotheses regarding the processes that regulate recruitment variation, we suggest that for cod and haddock on Georges Bank the two processes occur simultaneously (food limitation of the larval stages, and off-Bank losses due to the circulation). However, there are periods when one process may dominate. With the flow-field used in our model the results indicate that advective losses of the egg-stage are on the order of 10%. In the absence of predation, the dominant cause of mortality of the first-feeding larval stage (5–7 days post-hatch) is starvation. For the remainder of the larval stage

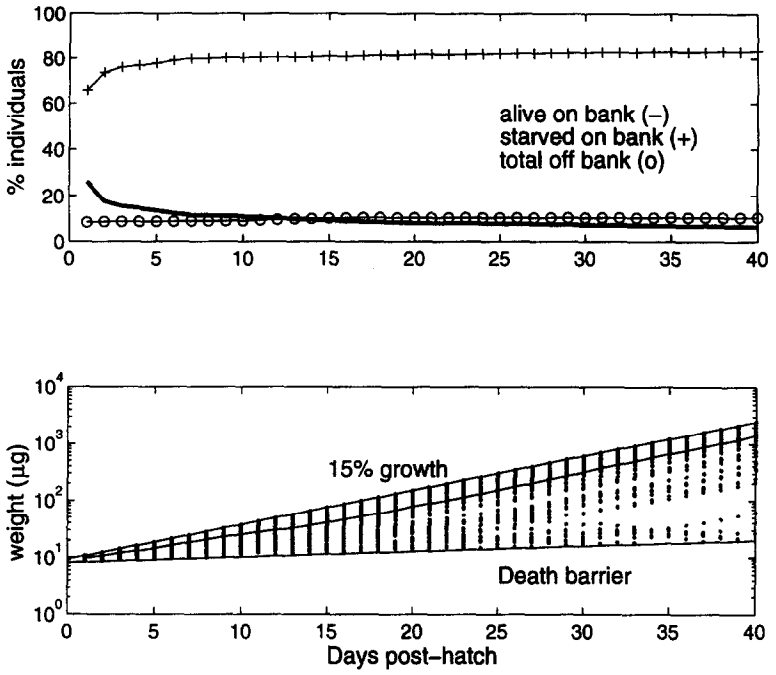

Fig. 18. Post-hatch time history of haddock larvae including a 5-fold increase of the egg, nauplii, C-I and C-II prey items and turbulence-enhanced contact rates showing, in the upper panel, the percentage of larvae alive (solid line), starved on-Bank (solid line with crosses), and advected off the Bank (solid line with open circles); and, in the lower panel, the daily size distribution (μg) for the live larvae on the Bank. Also indicated in the lower panel is the 15% per day growth curve, the death barrier and the mean weight of those larvae still on the Bank.

(at least to 40 days post-hatch), advective and starvation losses are similar (taking as our example the simulations that included turbulence). As noted above with reference to the eastern flank, this separation among biological and physical processes is somewhat artificial since in addition to causing direct losses by transport of larvae off the Bank, the circulation also can influence the growth and survival of larvae by moving them among areas of high and low concentrations of suitably-sized prey.

There are various important aspects that have not been dealt with at this stage in our model study of the Georges Bank cod and haddock larval populations. Those that need to be addressed include a more realistic description of the temporal and spatial distribution of the prey field, prey aggregation, the inclusion of larval behavior as a function of larval size, and consideration of temperature influences on the rates of physiological processes. These effects of temperature will be most important for model simulations that compare different seasons and years. Recent studies that examine the effect of turbulence on ingestion rates and on encounter rates as affected by larval swimming behavior within a range of turbulent conditions (MacKenzie *et al.*, 1994; MacKenzie and Kiørboe, 1995) also will need to be considered. Note that at present we have not considered the effect of predation as a process influencing the abundance of larvae on the Bank. Predation can be viewed as a system-wide

scaling factor, unless it is spatially-dependent; however, we have no information on the small-scale predation losses of larval cod and haddock on Georges Bank.

In these simulations we have considered only the effect of horizontal variations in prey concentration on larval growth. Analogous effects arising from vertical variations in the prey field concentration are likely and expected. Field studies have shown that stratification on Georges Bank can significantly influence the feeding and survival of larval cod and haddock (Buckley and Lough, 1987). In that study, up to 50% of haddock larvae (mean size 11.2 mm) from a well-mixed site in spring 1983 on Georges Bank were found to have RNA/DNA ratios in the range observed in the laboratory for starved larvae. These field observations support the hypothesis, and the model results, that haddock larvae require higher prey densities than cod and seem more adapted to spring conditions when prey are concentrated by stratification.

In order for larvae to survive and grow in the deterministic model simulations, the concentrations of the four smallest prey categories had to be increased 5-fold for cod and 15-fold for haddock. Although the inclusion of turbulence effects on contact rates removed this requirement for cod and reduced it (to 5-fold) for haddock, this variability of prey concentrations (up to five times) is not unrealistic, and is within the range observed by Lough (1984), Buckley and Lough (1987), and Incze *et al.* (1996). Buckley and Lough's studies found increased prey aggregations and peak densities of larvae in the vicinity of a pycnocline where the turbulence is minimum and thus the effect of enhanced contact rates may be weakest (see Figs 13–15). Lough and Mountain (1996), using the same data as Buckley and Lough (1987), found an interaction effect between prey density and turbulence levels for larval cod and haddock feeding in a stratified water column on the southern flank of Georges Bank. That is, the optimum feeding response (average number of prey per larvae) at high prey densities extended to lower densities at higher turbulence levels until it interfered with capture success (MacKenzie *et al.*, 1994). Lough and Mountain also found that the optimal feeding response depended on larval size. The aggregation of prey where there are *absolute* increases in prey concentrations may be particularly important to achieve the observed growth rates for haddock larvae. Recall that the ability to find and ingest prey by the smallest larvae was critical to achieving growth rates observed in the field (Figs 5 and 6). In this regard, two of the crucial parameters in the model are the concentration of prey separated into size categories and their distributions, especially for those sizes appropriate for the smallest larvae. Ideally, prey distribution should be known in detail horizontally and vertically throughout the Bank, but in practice it is poorly known at some locations and unknown at most places. Analyses of historical small-mesh plankton samples and new information collected during future field programs (GLOBEC, 1992; U.S. GLOBEC News, 1993) coupled with advances in zooplankton population advection–diffusion–reaction models (e.g. Franks, 1992; Lewis *et al.*, 1994; Wolff, 1994) should provide additional details.

A corollary to the observed coincidence of highest prey biomass and the mean depth of the larvae is that there may be a larval behavioral component that we have not included in the present formulation. It is possible that the increased larval biomass observed by Buckley and Lough (1987) is a result of only those larvae located in the pycnocline surviving, or it may be a result of vertically migrating larvae seeking out the regions where the prey are aggregated.

The individual based modeling (IBM) approach, which is a natural extension of Lagrangian particle-tracking descriptions of the circulation, is a useful tool in the study of the variability in feeding and growth characteristics of individual larvae. The approach

integrates the unique temporal and spatial history of the individual larvae, each of which is exposed to different prey concentrations and physical parameters. In this manner, the growth of individual larvae can be understood in terms of a detailed time-history of the food available to the larvae, which itself is a function of the unique trajectory of each larva through the prey field, and the ability to encounter (and capture) the prey, e.g. in our case as affected by the turbulence. Thus far we have only considered passive larvae, i.e. larvae that are advected in the flow. In Werner *et al.* (1993) we considered the effect of vertical (and horizontal) swimming behavior and found that behavior could significantly affect the fate of the larvae in terms of retention (or not) on the Bank. In view of the above statements on prey and larval aggregation, larval behavior will certainly play a role in the determination of the individuals' growth rates and will be examined in future studies.

In conclusion, the ability to couple a larval fish trophodynamics model with a detailed model of the physical circulation on realistic topography, both of which operate at the scale of individual larvae, is providing a new tool for the development and exploration of the critical hypotheses regulating the variability of marine fish populations on Georges Bank.

Acknowledgements—We wish to thank D. R. Lynch and M. M. Sinclair for insightful discussions, and B. O. Blanton for his help in various aspects of the particle tracking and the preparation of the figures. Two anonymous reviewers provided helpful comments on an earlier version of this manuscript. This research was supported by the joint NSF-NOAA U.S. GLOBEC Program and the Canadian Panel on Energy, Research and Development. This is contribution number 32 of the U.S. GLOBEC Program.

REFERENCES

Beyer J. E. and G. C. Laurence (1980) A stochastic model of larval growth. *Ecological Modelling*, **8**, 109–132.

Beyer J. E. and G. C. Laurence (1981) Aspects of stochasticity in modelling growth and survival of clupeoid fish larvae. *Rapports et Procés-Verbaux des Reunion Conseil Internationale Exploration de la Mer*, **178**, 17–23.

Bolz G. R. and R. G. Lough (1988) Growth through the first six months of Atlantic cod, *Gadus morhua*, and haddock, *Melanogrammus aeglefinus*, based on daily otolith increments. *Fisheries Bulletin, U.S.*, **86**, 223–235.

Brander K. M. (1994) The location and timing of cod spawning around the British Isles. *ICES Journal of Marine Science*, **51**, 71–89.

Brander K. M. and P. C. F. Hurley (1992) Distribution of early stage Atlantic cod, *Gadus morhua*, haddock *Melanogrammus aeglefinus*, and witch flounder *Glyptocephalus cynoglossus* eggs on the Scotian Shelf: a reappraisal of evidence on the coupling of cod spawning and plankton production. *Canadian Journal of Fisheries and Aquatic Sciences*, **49**, 238–251.

Buckley L. J. and R. G. Lough (1987) Recent growth, biochemical composition, and prey field of larval haddock (*Melanogrammus aeglefinus*) and Atlantic cod (*Gadus morhua*) on Georges Bank. *Canadian Journal of Fisheries and Aquatic Sciences*, **44**, 14–25.

Cushing D. H. (1983) Are fish larvae too dilute to affect the density of their food organisms? *Journal of Plankton Research*, **6**, 591–599.

Davis C. S. (1982) Fine-mesh (0.165 mm) zooplankton on Georges Bank between September 1974 and February 1979: Data report, Laboratory Reference Document, National Marine Fisheries Service, Northeast Fisheries Center, Woods Hole, MA, pp. 82–30.

Davis C. S. (1984a) Interaction of a copepod population with the mean circulation on Georges Bank. *Journal of Marine Research*, **42**, 573–590.

Davis C. S. (1984b) Predatory control of copepod seasonal cycles on Georges Bank. *Marine Biology*, **82**, 31–40.

Davis C. S. (1987) Zooplankton life cycles, In: *Georges Bank*, R. H. Backus and D. W. Bourne, editors, MIT Press, Cambridge, MA, pp. 256–267.

DeAngelis D. L. and L. J. Gross (editors) (1992) *Individual-based models and approaches in ecology*, Chapman and Hall, New York, 525 pp.

Franks P. J. S. (1992) Sink or swim: accumulation of biomass at fronts. *Marine Ecology Progress Series*, **82**, 1–12.

Gallager S. and I. H. von Herbing (1994) Zooplankton process studies: larval cod feeding and growth. In: Cruise Report, RV/ISELIN Cruise C19407 to Georges Bank, 25 May–16 June 1994, pp. 29–32.

Galperin B., L. H. Kantha, S. Hassid and A. Rosati (1988) A quasi-equilibrium turbulent energy model for geophysical flows. *Journal of Atmospheric Science*, **45**, 55–62.

GLOBEC (1992) Northwest Atlantic Implementation Plan, Report Number 6, 69 pp.

Hjort J. (1914) Fluctuations in the great fisheries of northern Europe. *Rapports et Procés-Verbaux des Reunion Conseil Internationale Exploration de la Mer*, **20**, 1–228.

Horne E. P. W., J. W. Loder, C. E. Naimie and N. S. Oakey (1996) Turbulence dissipation rates and nitrate supply in the upper water column on Georges Bank. *Deep-Sea Research II*, **43**, 1683–1712.

Incze L. S., P. Aas and T. Ainaire (1996) Distribution of copepod nauplii and turbulence on the southern flank of Georges Bank: implications for feeding by larval cod (*Gadus morhua*). *Deep-Sea Research II*, **43**, 1855–1873.

Kane J. (1984) The feeding habits of co-occurring cod and haddock larvae. *Marine Ecology Progress Series*, **16**, 9–20.

Laurence G. C. (1978) Comparative growth, respiration and delayed feeding abilities of larval cod (*Gadus morhua*) and haddock (*Melanogrammus aeglefinus*) as influenced by temperature during laboratory studies. *Marine Biology*, **50**, 1–7.

Laurence G. C. (1985) A report on the development of stochastic models of food limited growth and survival of cod and haddock larvae on Georges Bank. In: *Growth and survival of larval fishes in relation to the trophodynamics of Georges Bank cod and haddock*, G. C. Laurence and R. G. Lough, editors, NOAA Tech. Mem., NMFS-F/NEC-36, pp. 83–150.

Lewis C. V. W., C. S. Davis and G. Gawarkiewicz (1994) Wind-forced biological–physical interaction on an isolated offshore bank. *Deep-Sea Research II*, **41**, 51–73.

Loder J. W., K. F. Drinkwater, N. S. Oakey and E. P. W. Horne (1993) Circulation, hydrographic structure and mixing at tidal fronts: the view from Georges Bank. *Philosophical Transactions of the Royal Society of London Series A*, **343**, 447–460.

Lough R. G. (1984) Larval fish trophodynamic studies on Georges Bank: a sampling strategy and initial results. In: *The propagation of cod* Gadus morhua *L.*, E. Dahl, D. S. Danielssen, E. Moksness and P. Solemdal, editors, Flodevigen rapportser, Vol. 1, pp. 395–434.

Lough R. G. and D. G. Mountain (1996) Effect of small-scale turbulence on feeding rates of larval cod and haddock in stratified water on Georges Bank. *Deep-Sea Research II*, **43**, 1745–1772.

Lough R. G., W. G. Smith, F. E. Werner, J. W. Loder, F. E. Page, C. G. Hannah, C. E. Naimie, R. I. Perry, M. Sinclair and D. R. Lynch (1994) Influence of wind-driven advection on interannual variability in cod egg and larval distributions on Georges Bank: 1982 vs 1985. *ICES Marine Science Symposium Series*, **198**, 356–378.

Lough R. G. and D. C. Potter (1993) Vertical distribution patterns and diel migrations of larval and juvenile haddock, *Melanogrammus aeglefinus*, and cod, *Gadus morhua*, on Georges Bank. *Fisheries Bulletin, U.S.*, **91**, 281–303.

Lynch, D. R., J. T. C. Ip, C. E. Naimie and F. E. Werner (1996) Comprehensive coastal circulation model with application to the Gulf of Maine. *Continental Shelf Research*, **16**, 875–906.

MacKenzie B. R. and T. Kiørboe (1995) Encounter rates and swimming behavior of pause-travel and cruise larval fish predators in calm and turbulent environments, *Limnology and Oceanography*, **40**, 1278–1289.

MacKenzie B. R. and W. C. Leggett (1991) Quantifying the contribution of small-scale turbulence to the encounter rates between larval fish and their zooplankton prey: effects of wind and tide. *Marine Ecology Progress Series*, **73**, 149–160.

MacKenzie B. R., T. J. Miller, S. Cyr and W. C. Leggett (1994) Evidence for a dome-shaped relationship between turbulence and larval fish ingestion rates. *Limnology and Oceanography*, **39**, 1790–1799.

Mangel M. and C. W. Clark (1988) *Dynamic modeling in behavioral ecology*, Princeton Univ. Press, Princton, NJ, 308 pp.

Mellor G. L. and T. Yamada (1982) Development of a turbulence closure model for geophysical fluid problems. *Reviews of Geophysics and Space Physics*, **20**, 851–875.

Morse W. W. (1989) Catchability, growth and mortality of larval fishes. *Fisheries Bulletin, U.S.*, **87**, 417–446.

Muelbert J. H., M. R. Lewis and D. E. Kelley (1994) The importance of small-scale turbulence in the feeding of herring larvae. *Journal of Plankton Research*, **16**, 927–944.

Mullin M. M. (1993) *Webs and scales*, Washington Sea Grant Program, Seattle, WA, 135 pp.

Naimie C. E., J. W. Loder and D. R. Lynch (1994) Seasonal variation of the three-dimensional residual circulation on Georges Bank. *Journal of Geophysical Research*, **99**, 15,967–15,989.

Naimie C. E. (1995) On the Modeling of the Seasonal Variation of the Three-Dimensional Circulation Near Georges Bank. PhD Dissertation, Dartmouth College, Hanover, NH, 266 pp.

Naimie, C. E. (1996) Georges Bank residual circulation during weak and strong stratification periods—prognostic numerical model results. *Journal of Geophysical Research*, **101**, 6469–6486

Owen R. W. (1989) Microscale and finescale variations of small plankton in coastal and pelagic environments. *Journal of Marine Research*, **47**, 197–240.

Page F. H. and K. T. Frank (1989) Spawning time and egg-stage duration in Northwest Atlantic haddock (*Melanogrammus aeglefinus*) stocks with emphasis on Georges and Browns Bank. *Canadian Journal of Fisheries and Aquatic Sciences*, **46**, 68–81.

Parsons T. R., M. Takahashi and B. Hargrave (1984) *Biological oceanographic processes*, Pergamon Press, 330 pp.

Perry R. I. (1994) Book review of *Webs and scales*: Physical and ecological processes in marine fish recruitment. *Fisheries Oceanography*, **3**, 218–220.

Sinclair M. (1988) Marine Populations: An Essay on Population Regulation and Speciation, Seattle, WA, Washington Sea Grant Program, 252 pp.

Rothschild B. J. (1992) Application of stochastic geometry to problems in plankton ecology. *Philosophical Transactions of the Royal Society of London, Series B*, **336**, 225–237.

Rothschild B. J. and T. R. Osborn (1988) Small-scale turbulence and plankton contact rates. *Journal of Plankton Research*, **10**, 465–474.

Smith W. G. and W. W. Morse (1985) Retention of larval haddock *Melanogrammus aeglefinus* in the Georges Bank region, a gyre-influenced spawning area. *Marine Ecology Progress Series*, **24**, 1–13.

Sundby S. and P. Fossum (1990) Feeding conditions of Arcto–Norwegian cod larvae compared with the Rothschild and Osborn theory on small-scale turbulence and plankton contact rates. *Journal of Plankton Research*, **12**, 1153–1162.

Theilacker G. H., K. M. Bailey, M. F. Canino and S. M. Porter (1996) Variations in larval walleye pollock feeding and condition: a synthesis. *Fisheries Oceanography*, **5**, 112–123.

Tyler J. A. and K. A. Rose (1994) Individual variability and spatial heterogeneity in fish population models. *Reviews of Fish Biology and Fisheries*, **4**, 91–123.

U.S. GLOBEC News (1993) A pilot study of stratification variability on Georges Bank and its effect on larval fish survival, contributed by The Stratification Group, May issue.

Werner F. E., F. H. Page, D. R. Lynch, J. W. Loder, R. G. Lough, R. I. Perry, D. A. Greenberg and M. M. Sinclair (1993) Influences of mean advection and simple behavior on the distribution of cod and haddock early life stages on Georges Bank. *Fisheries Oceanography*, **2**, 43–64.

Winemiller K. O. and K. A. Rose (1993) Why do fish produce so many tiny offspring? *American Naturalist*, **142**, 585–603.

Wolff E. M. (1994) An advection–diffusion–reaction model with NPZ (nutrients, phytoplankton and zooplankton) relationships applied to Georges Bank, MSc Thesis, Dartmouth College, Hanover, NH.